Electric-field control and adiabatic evolution of shallow donor impurities in silicon

A. S. Martins, R. B. Capaz, and Belita Koiller
Instituto de Física, Universidade Federal do Rio de Janeiro, Caixa Postal 68.528, 21945-970, Rio de Janeiro, Brazil
(Received 27 August 2003; published 24 February 2004)

We present a tight-binding study of donor impurities in Si, demonstrating the adequacy of this approach for this problem by comparison with Kohn-Luttinger effective mass theory and experimental results. We consider the response of the system to an applied electric field: donors near a barrier material and in the presence of a uniform electric field may undergo two different ionization regimes according to the distance of the impurity to the Si/barrier interface. We show that for impurities ~ 5 nm below the barrier, adiabatic ionization is possible within switching times of the order of one picosecond, while for impurities ~ 10 nm or more below the barrier, no adiabatic ionization may be carried out by an external uniform electric field. Our results are discussed in connection with proposed Si:P quantum computer architectures.

DOI: 10.1103/PhysRevB.69.085320 PACS number(s): 71.55.Cn, 71.15.Ap, 03.67.Lx

I. INTRODUCTION

Simple donors in Si have recently become the subject of renewed interest due to proposals of quantum computer architectures in which P donors in Si play the role of qubits.[1–3] Logic operations in such architectures involve the response of the bound-electron wave functions to voltages applied to a combination of metal gates separated by a barrier material (e.g. SiO_2) from the Si host. The so-called *A*-gate, placed above each donor site, pulls the electron wave function away from the donor, aiming at partial reduction[1] or total cancellation[3] of the electron-nuclear contact coupling in architectures where the qubits are the ^{31}P nuclear spins. In a related proposal based on the donor-electron spins as qubits,[2] the gates drive the electron wave function into regions of different *g* factors, allowing the exchange coupling between neighboring electrons to be tuned. Ideally, electric-field control over the donor electron wave function requires all operations to be performed in the adiabatic regime,[4] which sets a lower bound for the time scales involved in such processes.

Recent studies have demonstrated that the tight-binding (TB) approach, traditionally adopted for deep levels,[5] provides a valid description for intermediate[6,7] and shallow levels[8] in semiconductors. Impurity states are calculated from a sequence of supercell sizes and a finite-size analysis which provides extrapolation to the bulk limit. Also, electric-field effects may be easily incorporated within the TB scheme,[9] allowing estimates of switching times in electric-field-tunable devices.[10] In this work we present a TB description for donors in Si, aiming at a physical description of the relevant properties involved in the *A*-gate operations mentioned above.

Donors in Si have been extensively and successfully investigated within the Kohn-Luttinger (K&L) envelope function approach,[11] thus providing a preliminary test for the TB approach by comparison of wave functions predicted by the two formalisms. This comparison is presented in the following section. In Sec. III we explore a simplified model of the *A*-gate operations in the Kane quantum computer proposal[1] by considering the Si:P system under a uniform electric field and near a barrier. In Sec. IV we discuss operation times and restrictions imposed by the donor positioning with respect to the Si/barrier interface in connection with the adiabaticity of the *A*-gate operations. Our summary and conclusions are presented in Sec. V.

II. TB DESCRIPTION FOR DONORS IN SILICON

A. Formalism

The TB Hamiltonian for the impurity problem is written as[6]

$$H=\sum_{ij}\sum_{\mu\nu} h_{ij}^{\mu\nu} c_{i\mu}^{\dagger} c_{j\nu} + \sum_{i,\nu} U(r_i) c_{i\nu}^{\dagger} c_{i\nu}, \qquad (1)$$

where i and j label the atomic sites, μ and ν denote the atomic orbitals and r_i is the distance of the site i to the impurity site. The matrix elements $h_{ij}^{\mu\nu}$ define all the on-site energies and first and second neighbors hoppings for the bulk material. The donor impurity potential $U(r_i)$ is described by a screened Coulomb potential ($\epsilon = 12.1$ for Si)

$$U(r_i) = -\frac{e^2}{\epsilon r_i}. \qquad (2)$$

At the impurity site ($r_i = 0$), the perturbation potential is assigned the value $-U_0$, a parameter describing central cell effects characteristic of the substitutional species. In the present calculations, U_0 was kept as an adjustable parameter (previous estimates for this parameter[6] are of the order of one to a few eV). We adopt here the sp^3s^* TB parametrization for Si proposed by Klimeck *et al.*,[12] which includes first and second neighbors interactions. Inclusion of hopping matrix elements up to second neighbors provides a good description of the effective masses at the conduction-band minima. This parametrization gives the *k*-space positions of the six band minima at the six equivalent points along the Δ lines, at $\Delta_{min} = 0.75(2\pi/a)$, where $a = 5.431$ Å is the conventional cubic lattice parameter for Si. We do not include spin-orbit corrections in our calculations, since our main concern here is on charge response to external electric fields. We have also verified that spin-obit corrections have negligible effect around the conduction-band minima, e.g., in the

 ©2004 The American Physical Society

effective masses. Spin-orbit effects must of course be included in models describing donor-electron spin response and control.

The eigenstates of H are determined for a system where a single impurity is placed in a cubic supercell containing $N=8L^3$ atoms arranged in the diamond structure, where L is the length of the supercell edge in units of a. The supercells are subject to periodic boundary conditions, and full numerical diagonalization can be performed for $L \lesssim 6$. Much larger supercells[8] (up to 10^6 atoms) may be treated within a variational scheme[13] where the ground-state wave function and binding energy E_L for a donor level is obtained by minimizing the expectation value of $\langle\Psi|(H-\varepsilon_{ref})^2|\Psi\rangle$. For the donor ground state, ε_{ref} is a reference energy chosen well within the gap, but nearest to the conduction-band minimum, and excited states are obtained by tuning ε_{ref} towards the conduction-band edge. Finite-size scaling allows extrapolation to the bulk limit ($L\to\infty$) according to the *ansatz*[6,7]

$$E_L = E_b + \tilde{E} e^{-L/\lambda}, \tag{3}$$

where E_b is the binding energy for a single donor in the bulk.

The eigenfunctions of Eq. (1) written in the basis of atomic orbitals $|\phi_\nu(\mathbf{r}-\mathbf{R}_i)\rangle$ are given by $|\Psi_{TB}(\mathbf{r})\rangle = \Sigma_{i\nu} a_{i\nu} |\phi_\nu(\mathbf{r}-\mathbf{R}_i)\rangle$ where the expansion coefficients $a_{i\nu}$ give the probability amplitude of finding the electron in the orbital ν localized at $\mathbf{R}_i$. We do not include explicit expressions for the atomic orbitals; the overall charge distribution is conveniently described through the TB envelope function squared,[14]

$$|\Psi_{EF}(\mathbf{R}_i)|^2 = \sum_\nu |a_{i\nu}|^2. \tag{4}$$

B. Donor ground state

In the proposed TB model, the only free parameter is related to the on-site value for the impurity potential U_0. In Fig. 1(a) we present the converged ($L\to\infty$) binding energy of the lowest donor state as a function of U_0. We also characterize the donor ground state by its orbital averaged spectral weight[14] at Δ_{min},

$$W(\Delta_{min}) = \frac{2}{N} \sum_{\mu=1}^{6} \sum_{ij\nu} e^{i\mathbf{k}_\mu\cdot(\mathbf{R}_i-\mathbf{R}_j)} a_{i\nu} a_{j\nu}, \tag{5}$$

where N is the number of atomic sites in the supercell, and the first summation is over the six equivalent $\mathbf{k}_\mu$ at the conduction-band minima. This quantity is plotted in Fig. 1(b) as a function of U_0.

We determine the value of U_0 so that the binding energy of the donor results to be in good agreement with the experimental value which, for P in Si, is $E_b = 45.6$ meV. As indicated in Fig. 1, $U_0 = U_P \cong 1.48$ eV gives the correct binding energy for the P donors in Si. This value for U_0 is used in the calculations below.

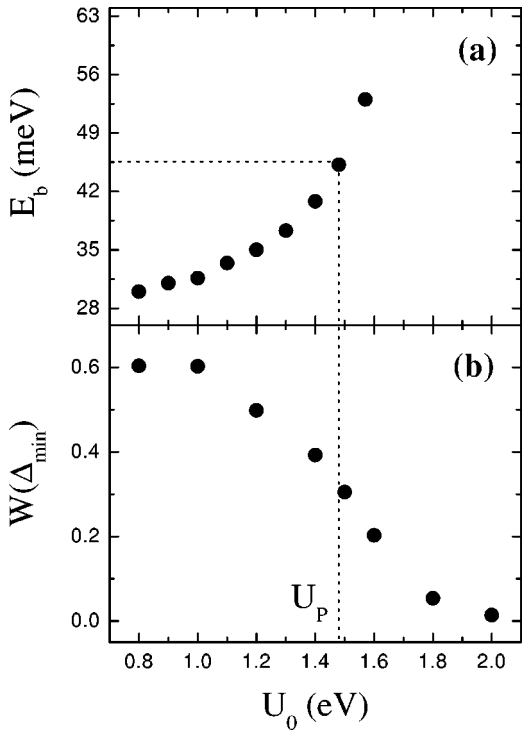

FIG. 1. (a) Binding energy of the ground impurity state as a function of the on-site perturbation strength U_0, obtained from the $L\to\infty$ extrapolation ansatz. The dotted line indicates the value $U_0 = U_P$ that reproduces the experimental Si:P A_1 state binding energy. (b) Calculated spectral weight at the conduction-band edge for the ground state. Note that as the perturbation U_0 becomes weaker, E_b approaches the K&L binding energy, while W does not approach 1.

C. Comparison with Kohn-Luttinger effective mass theory

Effective mass theory (EMT) exploits the duality between real and reciprocal space, where delocalization in real space leads to localization in k space, e.g., for shallow donors around the k vector at the minimum of the conduction band. Within EMT in its simplest formulation (single-valley approximation),[11] the ground state for donors in Si is sixfold degenerate, due to the sixfold degeneracy of the Si conduction band. As noted originally by K&L, valley-orbit interactions[15] lead to a nondegenerate ground-state envelope of A_1 symmetry,[11,16]

$$\psi(\mathbf{r}) = \frac{1}{\sqrt{6}} \sum_{\mu=1}^{6} F_\mu(\mathbf{r}) \phi_\mu(\mathbf{r}), \tag{6}$$

where $\phi_\mu(\mathbf{r}) = u_\mu(\mathbf{r}) e^{i\mathbf{k}_\mu\cdot\mathbf{r}}$ are the pertinent Bloch wave functions, and the envelope functions given by (e.g., for $\mu = z$)[11]

$$F_z(\mathbf{r}) = \frac{1}{\sqrt{\pi a^2 b}} e^{-[(x^2+y^2)/a^2 + z^2/b^2]^{1/2}}. \tag{7}$$

The effective Bohr radii for Si from a variational calculation are $a = 2.51$ nm and $b = 1.44$ nm.[17] In Fig. 2 we present the TB envelope function squared calculated from Eq. (4) along three symmetry directions with the corresponding K&L re-

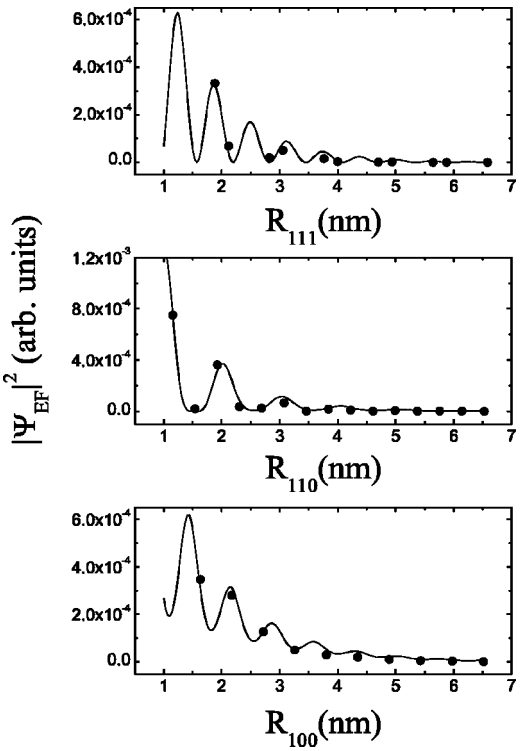

FIG. 2. The dots give the TB envelope function squared for the lowest impurity state along three high-symmetry directions. The lines are the corresponding K&L $|\psi|^2$ results. Note that the TB approach captures the oscillations of the K&L wave function in the asymptotic region.

sults obtained from Eq. (6), where the periodic part of the Bloch functions have not been explicitly included, consistent with not explicitly including the atomic orbitals in the TB description. Note that the oscillatory behavior coming from the interference among the plane-wave part of the six ϕ_μ is well captured by the TB envelope function at the atomic sites, where it is defined [see Eq. (4)].

The good agreement between TB and K&L is limited to distances from the impurity site larger than a few lattice parameters (~ 1 nm). Closer to the impurity, particularly at the impurity site, the TB results become much larger than the K&L prediction, in qualitative agreement with experiment.[11] This reflects central-cell effects, not included in the K&L expressions (6) and (7). In the central-cell region, the discrepancy between TB and K&L wave functions is significantly larger than those reported for donors in GaAs,[8] a result that could have been anticipated from the spectral weight given in Fig. 1(b). EMT rests on the assumption that the impurity eigenstate is highly localized in k space, so that only Bloch states near the conduction-band minima enter in the expansion, as implied in Eq. (6). This is the case for GaAs,[8] where for a range of values of U_0 ($U_0 < 1.8$ eV) we find $W(\Gamma)$ essentially equal to one, in agreement with the EMT assumption. In Si, even small values of U_0 yield spectral weights at Δ_{min} well below one. For $U_0 = U_P$ in particular, $W(\Delta_{min}) \cong 0.3$.

We remark that the sharp shallow-to-deep transition obtained for GaAs in Ref. 8, with kinks in the curves of E_b and W versus U_0, is not reproduced here (see Fig. 1). We attribute this to the lack of a strictly shallow region, with the spectral weight of the donor state concentrated in one or a few k points. Therefore, while the binding energy of shallow donors in GaAs is essentially constant, independent of the species (~ 6 meV for C, Si, and Ge, in excellent agreement with the EMT estimate), in Si it varies according to the donor species (45 meV for P, 53 meV for As, and 42 meV for Sb, to be compared with the K&L single-valley estimate of 30 meV). It is interesting to note in Fig. 1(a) that, as the impurity level becomes shallower by decreasing U_0, E_b approaches the K&L single-valley estimate for the binding energy.[11]

III. DONORS IN SILICON UNDER A UNIFORM ELECTRIC FIELD

The formalism presented in Sec. II is easily extended to include a uniform electric field in the system. Assuming a constant field **E** applied along the $[00\bar{1}]$ direction, it is incorporated in the TB formalism by modifying the on-site energies in Eq. (1) as follows:[9,10]

$$h_{ii}^{\nu\nu}(E) = h_{ii}^{\nu\nu}(0) - |e| E z_i . \tag{8}$$

Periodic boundary conditions lead to a discontinuity in the potential at the supercell boundary $z_i = Z_B$, where Z_B is half of the supercell length along [001] or, equivalently, the distance from the impurity to the Si/barrier interface. The potential discontinuity, $V_B = 2|e|EZ_B$, actually has a physical meaning in the present study: It models the potential due to the barrier material layer above the Si host[1] (see inset in Fig. 3).

A description for the A-gate operations may be inferred from the behavior of the TB envelope function squared at the impurity site under applied field E, normalized to the zero-field value:

$$A/A_0 = |\Psi_{EF}^{E}(0)|^2 / |\Psi_{EF}^{0}(0)|^2 . \tag{9}$$

The notation here indicates that this ratio should follow a behavior similar to that for the hyperfine coupling constants between the donor nucleus and electron with (A) and without (A_0) external field. Since the hyperfine interaction A is proportional to $|\Psi(0)|^2$, and we are using here the envelope rather than the full TB eigenfunctions, this equivalence is not rigorous. The ratio in Eq. (9) is plotted in Fig. 3(a) for three values of the impurity depth with respect to the Si/barrier interface. Calculations for $Z_B = 10.86$ nm were performed with cubic supercells ($L = 40$), while for $Z_B = 5.43$ and 21.72 nm tetragonal supercells with $L_x = L_y = 40$ and $L_z = 20$ and 80, respectively, were used. At small field values we obtain a quadratic decay of A/A_0 with E, in agreement with the perturbation theory results for the hydrogen atom.[18] At large enough fields, $|\Psi_{EF}^{E}(0)|^2$ becomes vanishingly small, and the transition between the two regimes is qualitatively different according to Z_B: For the largest values of Z_B we get an abrupt transition at a critical field E_c, while smaller Z_B (e.g., $Z_B = 5.43$ nm) lead to a smooth decay, similar to the one depicted in Ref. 1. In this latter case, we define E_c as the

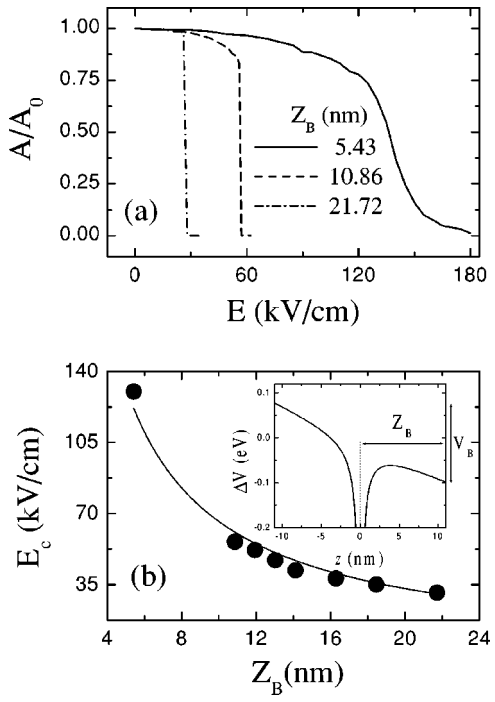

FIG. 3. (a) TB envelope function squared at the impurity site under applied field E, normalized to the zero-field value, for the indicated values of the impurity-Si/barrier interface distance Z_B. (b) Dependence of the critical field E_c on Z_B. The solid line is a best fit of the form $E_c \propto 1/Z_B$. The inset gives a schematic representation of the perturbation potential added to the bulk Si Hamiltonian due to the impurity at $\mathbf{R}=0$ and to a uniform electric field in the negative z direction.

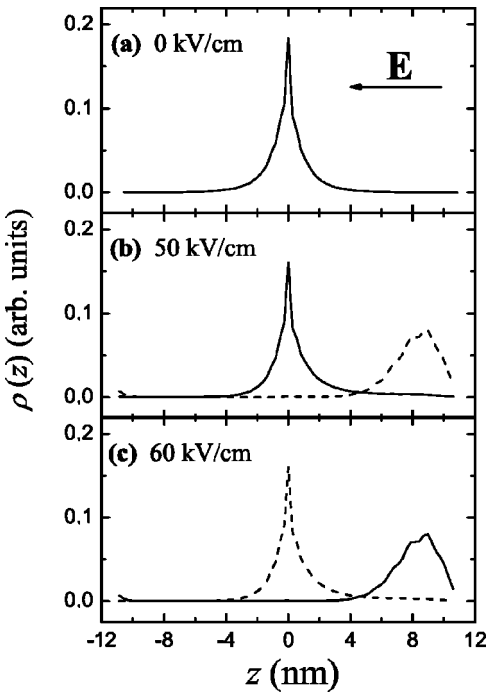

FIG. 4. Tight-binding envelope function squared projected along z for $Z_B=10.86$ nm and the indicated values of the field E applied in the negative z direction. The solid (dashed) line gives the donor ground (1st excited) state. Note in (b) and (c) the exchange among the $\rho(z)$ for the lowest energy states [*ground*] $\leftrightarrow$ [*excited*] which occurs over a narrow rage of electric field increase, a signature of the crossing behavior in Fig. 5(a).

field for which the curve A/A_0 versus E has an inflection point, where $A/A_0 \sim 0.5$, thus $E_c(5.43\ \text{nm}) = 130$ kV/cm. We find that the decrease of E_c with Z_B follows a simple rule $E_c \propto 1/Z_B$, as given by the solid line in Fig. 3(b).

The existence of two ionization regimes according to the donor depth was recently obtained within EMT by Kettle *et al.*[19] and by Smit *et al.*[20] In order to analyze the different regimes illustrated in Fig. 3(a), we study the overall behavior of the envelope squared profile along the z axis,

$$\rho(z) = \sum_{s=1}^{2} \sum_{x_i^s y_i^s} |\Psi_{EF}^{E}(\mathbf{R}_i^s)|^2, \tag{10}$$

where the first summation is over the two fcc sublattices, with $\mathbf{R}_i^s$ corresponding to the atomic sites in sublattice s, thus z labels each monolayer in the diamond structure, and $\rho(z)$ quantifies the z-projected charge distribution for the electron states under applied field E. Figure 4 gives $\rho(z)$ for the electron ground state and also for the first excited state with $Z_B = 10.86$ nm as the applied field increases. Up to fields very close to $E_c(\sim 53$ kV/cm), the ground-state distribution retains essentially the bound donor character, with the electronic charge accumulating predominantly around the impurity ($z=0$). For $E > E_c$ we observe an abrupt charge transfer towards the barrier, with some residual charge remaining at the impurity site. The first excited state displays a complementary behavior, with charge transfer from the barrier into the impurity region as E increases. The binding energies (energy eigenvalues relative to the bottom of the conduction band) are calculated here taking into account the dependence of the conduction-band edge under applied field. The binding energies of the two lowest electron states are given in Fig. 5(a). Note that they cross at E_c.

The binding energies of the two lowest eigenstates for $Z_B = 5.43$ nm are presented in Fig. 5(b). They do not cross, but rather display an anticrossing behavior, confirmed by the corresponding doubled-peaked charge distributions in Fig. 6, with wave functions extending over the attractive wells of the impurity and of the electric-field potential. This is consistent of eigenstates which are superpositions of bound states in each potential well. Note that for $E = E_c$ in Fig. 6(c), the two states have essentially the same charge distribution, as expected at the anticrossing point. The anticrossing in Fig. 5(b) is such that for $E < E_c$ the lines giving the two states are essentially parallel, converging asymptotically at zero field to the binding energies 45.6 meV, for the A_1 ground state, and 32.4 meV for the first excited state. This is very close to the experimental binding energy of the excited E (32.6 meV) and T_2 (33.9 meV) states, which cannot be individually resolved within our variational scheme.[16] Note that this was independently obtained with the same value of the parameter U_0, chosen to fit the A_1 state binding energy alone. Near and above E_c a typical two-level anticrossing behavior is ob-

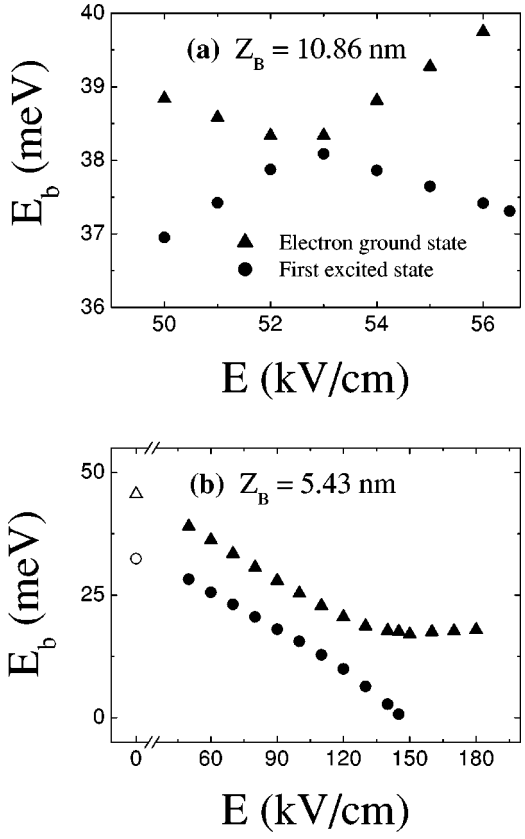

FIG. 5. Calculated binding energies vs electric-field intensity of the two lowest donor-electron states. (a) For $Z_B = 10.86$ nm the energies reveal a crossing regime. (b) Anticrossing of the two lowest electron states for $Z_B = 5.43$ nm. The open symbols correspond the zero-field calculated values: 45.6 meV and 32.4 meV.

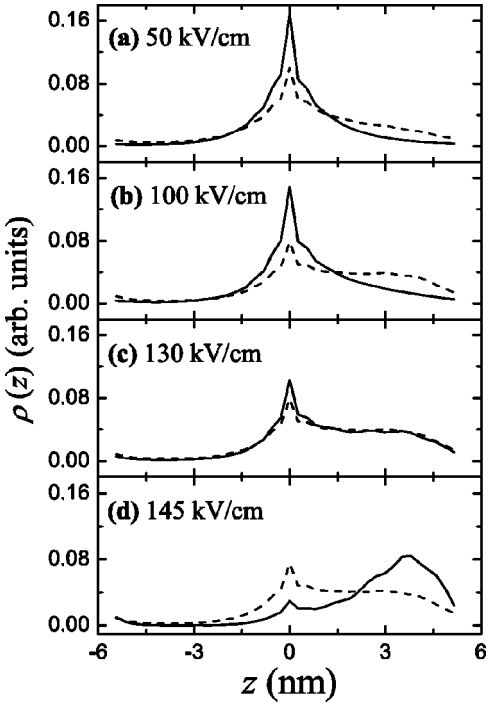

FIG. 6. TB envelope function squared projected along z for $Z_B = 5.43$ nm and the indicated values of the applied field E. The solid (dashed) line gives the ground (1st excited) state. At the critical field in (c) the two states have similar charge distributions, typical of a superposition of states localized in each well and a signature of the anticrossing behavior in Fig. 5(b).

tained, with the excited state eventually merging into the conduction band at $E = 150$ kV/cm.

The above results may be understood within a simple picture of the electron in a double-well potential, the first well being most attractive at the impurity site, $V(\mathbf{R}=0) = -U_0$, and the second well at the barrier interface, $V(z=Z_B) = -V_B/2 = -|e|EZ_B$ neglecting the Coulomb potential contribution (2) at the interface. An internal barrier separates the two wells and, for a fixed E, this internal barrier height and width increase with Z_B. Deep donor positioning leads to a weaker coupling between the states localized at each well, even close to level degeneracy, resulting the level crossing behavior illustrated in Fig. 5(a). For donor positioning closer to the interface the internal barrier gets weaker, enhancing the coupling between levels localized in each well and leading to wave function superposition and to the anticrossing behavior illustrated in Fig. 5(b). The scaling of E_c with $1/Z_B$ may also be understood assuming that the critical field corresponds to the crossing of the ground-state energies of two wells: The Coulomb well and an approximately triangular well at the barrier. Since the relative depths of the wells increases with EZ_B, and assuming that the ground-states energies are fixed with respect to each well's depth, leads to the $E_c \propto 1/Z_B$ behavior.

IV. ADIABATIC PROCESSES DRIVEN BY A UNIFORM ELECTRIC FIELD

Coherent manipulation of electrons by the *A*-gates requires that the switching time between different electron states be slow enough to guarantee adiabaticity of the process. Instantaneous eigenstates of $H(t)$ may thus be defined at any time t. In the present case, we assume a linear increase of the external field from 0 to a maximum value $E_{\max}$ so that $H(t) = H(0) - |e|E_{\max}zt$, with $0 < t < T$, where T is the total switching time. A lower bound for T is obtained from the adiabatic theorem,[4,21] following Ref. 10

$$T_a = \frac{\hbar |e| E_{\max} Z_B}{g_{\min}^2}, \tag{11}$$

where $g_{\min}$ is the minimum gap between the two lowest electron states. In the anticrossing case illustrated in Fig. 5(b), we get $g_{\min} \cong 9.8$ meV. Assuming that a totally ionized state is required as the final state, we take $E_{\max} = 180$ kV/cm, leading to $T_a \sim 0.5$ ps. This is a perfectly acceptable time for the operation of *A*-gates in spin-based Si quantum computer, given the relatively long electron-spin coherence times (of the order of a few ms) in Si.[22]

As the impurity distance from the barrier increases, one eventually reaches the crossing regime, when $g_{\min} \to 0$, meaning that $T_a \to \infty$ and no adiabatic ionization is possible. Ionization would still occur for $E > E_c$, but as a stochastic decay process from the first excited state. From Fig. 3(a) we see

that the *A*-gate might be used to partially reduce the contact interaction, in the case of $Z_B = 10.86$ nm to about 20% of its value at zero field. For larger Z_B the range for adiabatic variation in A/A_0 is even smaller. Therefore $Z_B \sim 5$ nm seems to be a favorable positioning for the donors, since it allows adiabatic reduction of A/A_0 to any desired final value, with this ratio varying smoothly from one (at $E=0$) to zero (for $E=E_{\max} \sim 2E_c$).

V. SUMMARY AND CONCLUSIONS

We have presented a TB study of donor levels in Si. The reliability of the TB approach for the present study was verified by comparison of the TB and K&L (Ref. 11) envelope functions in the asymptotic regime, as well as by the value predicted for the $A_1 - \{E, T_2\}$ energy splitting in agreement with experiment within our numerical accuracy. Previous TB studies of intermediate and shallow impurity levels in semiconductors[6–8] dealt with materials with band extrema at $\mathbf{k}=0$, and the present results show that the oscillatory behavior of the wave function due to interference effects in the plane-wave part of the Bloch wave functions, typical of degenerate band extrema at $\mathbf{k} \neq 0$, is well captured by the TB approach. Recent EMT studies focused primarily on donor ionization processes,[19,20] and were based on single-valley hydrogenic trial wave functions, leading to results qualitatively similar to those reported here in terms of the possible ionization behaviors.

In the presence of an increasing uniform electric field, the donor states respond in different ways according to the donor depth Z_B below the Si/barrier interface. For deeply positioned donors, i.e, for $Z_B \gg a, b$, where a and b are the Bohr radii for P in Si, abrupt ionization occurs at a critical field E_c, while for Z_B greater but of magnitude comparable to the Bohr radii, a smooth electronic charge transfer from the donor site towards the barrier interface is obtained, eventually leading to complete ionization. The different regimes were identified in three ways: (i) From the decrease in electronic charge at the donor nucleus [Fig. 3(a)]. This behavior implies an analogous dependence of the electron-nucleus hyperfine coupling constant A as a function of the increasing external field. (ii) From charge distributions (Figs. 4 and 6), where the superposition of donorlike and barrierlike bound states is inhibited for deeply positioned donors. (iii) From the behavior of the binding energies of the two lowest electron states as the applied field increases (Fig. 5), changing from a level crossing into an anticrossing regime as Z_B decreases. The donor excited states in the S-like manifold also play a role in the anticrossing regime, as illustrated for $E \lesssim E_c$ in Fig. 5(b).

The minimum gap $g_{\min}$ in the anticrossing regime is a key ingredient determining the possibility of an adiabatic evolution of the electron state under the action of the *A*-gates. Given that the product $E_c Z_B$ is approximately constant [see fit Fig. 3(b)], the *adiabatic* time T_a in (11) is expected to depend very weakly in the product $E_{\max} Z_B$, assuming one aims at complete ionization.[3] Therefore T_a should not depend explicitly on Z_B, but only implicitly through $1/g_{\min}^2$. We have shown that for $Z_B \sim 5$ nm, i.e., about twice the largest Bohr radius a in Eq. (7), electric field switching times smaller than 1 ps may be reached, which is a favorable operation time given the long electronic spin coherence times in Si. If one aims at a final state where only partial reduction of the electronic charge at the nucleus occurs,[1,2] values of Z_B of this order of magnitude are still the most convenient, since any final value of the nuclear charge may be attained.

The Bloch phases interference behavior in the donor wave functions has been previously shown to lead to oscillatory behavior of the exchange coupling between two donors,[17] affecting the two-qubit operations in exchange-based architectures in Si. We remark that such oscillations are well captured in the TB wave functions, and that the present study demonstrates that electric-field control over single donor wave functions, such as proposed in *A*-gate operations,[1–3] do not present additional complications due to the Si band structure. The only critical parameter is the donor positioning below the Si/barrier interface, which should be chosen and controlled according to the physical criteria presented here.

ACKNOWLEDGMENTS

We thank Daniel Loss and Bruce Kane for interesting discussions. We also thank Fabio Ribeiro for useful suggestions. This work was partially supported by Brazilian agencies CNPq, CAPES, FAPERJ, FUJB, PRONEX-MCT, and Instituto do Milênio de Nanociências-CNPq.

[1] B.E. Kane, Nature (London) **393**, 133 (1998).
[2] R. Vrijen, E. Yablonovitch, K. Wang, W.H. Jiang, A. Balandin, V. Roychowdhury, T. Mor, and D. DiVicenzo, Phys. Rev. A **62**, 012306 (2000).
[3] A.J. Skinner, M.E. Davenport, and B.E. Kane, Phys. Rev. Lett. **90**, 087901 (2003).
[4] A. Messiah, *Quantum Mechanics* (Dover, New York, 1999).
[5] H.P. Hjalmarson, P. Vogl, D.J. Wolford, and J.D. Dow, Phys. Rev. Lett. **44**, 810 (1980).
[6] J.G. Menchero, R.B. Capaz, B. Koiller, and H. Chacham, Phys. Rev. B **59**, 2722 (1999).
[7] J.G. Menchero and T.B. Boykin, Phys. Rev. B **59**, 8137 (1999).
[8] A.S. Martins, J.G. Menchero, R.B. Capaz, and B. Koiller, Phys. Rev. B **65**, 245205 (2002).
[9] M. Graf and P. Vogl, Phys. Rev. B **51**, 4940 (1995).
[10] F.J. Ribeiro, R.B. Capaz, and B. Koiller, Appl. Phys. Lett. **81**, 2247 (2002).
[11] W. Kohn, in *Solid State Physics–Advances in Research and Applications*, edited by F. Seitz and D. Turnbull (Academic Press, New York, 1957), Vol. 5, p. 257.
[12] G. Klimeck, R.C. Bowen, T.B. Boykin, C.S. -Lazaro, T.A. Cwik, and A. Stoica, Superlattices Microstruct. **27**, 77 (2000).

[13] R.B. Capaz, G.C. de Araujo, B. Koiller, and J.P. von der Weid, J. Appl. Phys. **74**, 5531 (1993).

[14] T.G. Dargam, R.B. Capaz, and B. Koiller, Phys. Rev. B **56**, 9625 (1997).

[15] A. Baldereschi, Phys. Rev. B **1**, 4673 (1970).

[16] The sixfold degenerate S-like donor states in Si split into three components due to the tetrahedral symmetry of the host: A non-degenerate ground state of A_1 symmetry given in Eq. (6), an excited triplet of symmetry T_2 followed by an excited doublet of symmetry E. The TB treatment adopted here correctly describes the symmetry and ordering of the states within this manifold when full diagonalization of the TB Hamiltonian is performed. Within the variational scheme we have not resolved the nearly degenerate T_2 and E levels, which are only 1.3 meV apart.

[17] B. Koiller, X. Hu, and S. Das Sarma, Phys. Rev. Lett. **88**, 027903 (2002).

[18] L.I. Schiff, *Quantum Mechanics* (McGraw-Hill, New York, 1968).

[19] L.M. Kettle, H.-S. Goan, S.C. Smith, C.J.W.L.C.L. Hollenberg, and C.I. Pakes, Phys. Rev. B **68**, 075317 (2003).

[20] G. Smit, S. Rogge, J. Caro, and T. Klapwijk, Phys. Rev. B **68**, 193302 (2003).

[21] E. Farhi, J. Goldstone, S. Gutmann, J. Lapan, A. Lundgren, and D. Preda, Science **292**, 472 (2001).

[22] R. de Sousa and S. Das Sarma, Phys. Rev. B **68**, 115322 (2003).